J. Comput. Appl. Res. Mech. Eng. Vol. 11. No. 1, pp. 257-277, 2021 DOI:10.22061/JCARME.2020.6370.1809

Journal of Computational and Applied Research in Mechanical Engineering

jcarme.sru.ac.ir

SRTTU

JCARME

ISSN: 2228-7922

Research paper

Bending of exponentially graded plates using new HSDT

Bathini Sidda Reddy[a,*], Ch. Ravikiran[b] and K. Vijaya Kumar Reddy[c]

[a]*Department of Mech. Engg., Rajeev Gandhi Memorial College of Engg.,and Tech., Nandyal, Kurnool (Dt), Andhra Pradesh, India-518 501.*

[b]*Department of Mech. Engg., MLR Institute of Technology, Telangana, India-500043*

[c]*Department of Mech. Engg., JNTUH, Telangana, India-500085*

Article info:

Article history:

Received: 02/01/2020

Revised: 12/11/2020

Accepted: 14/11/2020

Online: 17/11/2020

Keywords:

EGM plate,

Bending analysis,

Navier's method,

Thermal and mechanical loading,

Novel theory.

***Corresponding author:**

sidhareddy_548@rediffmaail.com

Abstract

The present paper considers the devise and development of a novel theory to examine the flexure analysis of exponentially graded plates exposed to thermal and mechanical loads. The properties such as elastic modulus and thermal modulus are assumed to vary exponentially along the thickness by keeping the poisson's ratio constant. This theory fulfills the nullity conditions on the upper and lower sides of the exponentially graded plates for transverse shear stress. Hamilton's principle is used to derive the equation of motion. The present theory's numerical results are assessed with three-dimensional elasticity solutions and the results of other authors available in the literature. The influence of thermomechanical loads, thickness ratios, and aspect ratios on the bending response of exponentially graded plates are studied in detail. The analytical formulations and solutions presented herein could provide engineers with the potential for the design and development of exponentially graded plates for advanced engineering applications.

1. Introduction

Functionally graded materials (FGMs) are advanced materials whose properties are assorted in a predetermined manner to enhance the overall structural functioning. Nowadays, FGMs are substitute materials in several structural applications used in situations where the operating conditions are severe.

Typically, FGMs are fabricated by mixing two different material phases with continuous composition gradation. Such gradation gives smooth variation in material properties. Most plate structures are normally exposed to thermal and mechanical loads. In fact, the FGM plates and shells are used to resist high-temperature environments. Conversely, the heterogeneity and widespread utilization of FGMs in structural members require the necessity to develop simple and precise theoretical models to understand the behaviour of the structures.

In the past, many authors have paid great effort in modeling the composite/sandwich plates and introduced various plate theories to study the FGMs behavior. Reddy and Chin [1], Zenkour [2-4], Kant et al. [5-9], Kadkhodayan [10], Matsunaga [11, 12], Xiang [13], Sidda Reddy et al. [14, 15] and Suresh Kumar et al. [16] used third-order displacement terms in the thickness direction to develop the higher order theory.

Mohammad and Singh [17] presented the theoretical formulations to explore the thermomechanical study of FGMPs. Thermo-bending problems of sandwich plates made of FG (FGSPs) were explored by Zenkour and Alghamdi [18], assuming that the sandwich plate faces are isotropic. Mechab et al. [19] analyzed the flexural behavior of FGPs. Carrera et al. [20] examined the single-layered and multilayered FG plates and shells. Daouadji et al. [21] investigated the static behavior of FG plates. Neves et al. [22] analyzed FGM plates for the static analysis. Zenkour [23] investigated the exponentially graded plates for static problems under transverse load using both 2-D plate theory through using trigonometric function (TPT) and three-dimensional solutions. Mantari and Soares [24, 25] explored the static behavior of exponentially graded plates (EGPs). Neves et al. [26] derived an HSDT to the static and eigenproblems of FGPs. Praveen and Reddy [27] investigated the transient analysis based on the nonlinear condition of FGPs under thermal loading using FEM. The bending behavior of temperature-dependent FGPs resting on an elastic foundation under thermomechanical load was investigated by Attia et al. [28]. A simple and refined n^{th} order SDPT was developed to investigate the mechanical and thermal buckling behavior of FGPs. [29]. The thermal buckling analysis of cross-ply laminated composite plates using a simplified HSDT was investigated by Chikh et al.[30] El-Haina et al.[31] presented ab analytical approach to examine the thermal buckling behavior of thick FGSPs. Menasria et al. [32] chose an undetermined integral-based displacement function for examining the thermal buckling of FGSPs. Beldjelili et al. [33] studied the hygro-therm-mechanical bending behavior of FGPs. The vibration behaviour of the nanosize FGPs considering the quasi 3D HSDT was developed by Boutaleb et al. [34]. A simple quasi-3D HSDT was developed by Boukhlif et al. [35] to investigate the fundamental frequencies of FGPs.

Bouanati et al. [36] used an efficient quasi 3D HSDT to explore the vibration behavior and wave propagation of triclinic/orthotropic plates. An efficient beam theory was used by Ait Atmane et al. [37] to analyze the static analysis of FGS beams with porosity considering the elastic foundations. Benahmed et al. [38] used hyperbolic theory to explore the static behavior of FGP resting on elastic foundation considering the thickness stretching. Karami et al. [39] presented a quasi-three dimensional theory to wave dispersion behavior for nano FGPs resting on an elastic foundation under a hygrothermal environment. Zaoui et al. [40] analyzed the vibration of FGPs rests on elastic foundation using quasi-three dimensional theory. Bouhadra et al. [41] developed an improved HSDT considering the stretching effect in FGPs. Younsi et al. [42] examined the static behavior of FG plates based on hyperbolic shape function considering the thickness stretching influence. Abualnour et al. [43] explored the frequency behavior of the FGPs with all edges that are simply support.

In this paper, a novel theory is proposed and formulated to the bending response of EGPs subjected to thermo-mechanical loads. The physical properties varied exponentially along with thickness direction. The equation of motion is derived using Hamilton's principle. The present results are compared with three-dimensional solutions. The influence of thermal and mechanical loads, thickness ratio, and aspect ratios on the bending response of EGPs are studied in detail. The analytical formulations and solutions presented herein could provide engineers with the potential for the design and development of exponentially graded plates for advanced engineering applications.

2. Formulation of novel theory

The physical dimensions of the rectangular plate with the adopted coordinate system are shown in Fig.1. The plate is composed of entirely ceramic material at the top side and graded to the bottom side ($z=-h/2$) that contains entirely metallic material. The elastic modulus and thermal

modulus of the FG plate vary exponentially along the thickness using Eq. (1), and Poisson's ratio (υ) is assumed to be constant.

$$P(z) = Exp\left[p\left(\frac{z}{h}+\frac{1}{2}\right)\right]P_b \qquad (1)$$

When p=0, it represents the property at the bottom surfacem and z=+h/2 represents the property at the top surface, i.e.: $P_t = P_b Exp[p]$.

2.1. Displacement field

The following is the displacement function which is proposed for the first time.

$$u = u_0 + z[f^* \psi_x - w_{,x}] + f(z)\psi_x \qquad 2(a)$$

$$v = v_0 + z[f^* \psi_y - w_{,y}] + f(z)\psi_y \qquad 2(b)$$

Kxml. $w = w$ 2(c)

where, $f^* = \text{hav}(r/2) + \sin(r/2)/4$ 2(d)

and $f(z) = z\,\text{hav}(rz/h)$ 2(e)

The Haversine function is simply written as *hav ( )* in Eq. 2(d-e). The in-plane displacement function is dependent on "r" and must be chosen. The optimal value of "r" is calculated after numerous computations from Eq. 8(a-f).

2.2. Strain-displacement relations

For the proposed displacement field, the strain and displacements are expressed in Eq. 2(a-d).

$$\begin{Bmatrix}\varepsilon_{xx}\\ \varepsilon_{yy}\\ \varepsilon_{xy}\end{Bmatrix} = \begin{Bmatrix} u_{0,x}\\ v_{0,y}\\ u_{0,y}+v_{0,x}\end{Bmatrix} + z\begin{Bmatrix} f^*\psi_{x,x} - w_{,xx}\\ f^*\psi_{y,y} - w_{,yy}\\ f^*(\psi_{x,y}+\psi_{y,x}) - 2w_{,xy}\end{Bmatrix}$$

$$+ f(z)\begin{Bmatrix}\psi_{x,x}\\ \psi_{y,y}\\ \psi_{y,x}+\psi_{x,y}\end{Bmatrix} = \varepsilon + zk + f(z)k^1 \qquad 3(a)$$

$$\begin{Bmatrix}\gamma_{yz}\\ \gamma_{xz}\end{Bmatrix} = \begin{Bmatrix} f^*\psi_y\\ f^*\psi_x\end{Bmatrix} + f'(z)\begin{Bmatrix}\psi_y\\ \psi_x\end{Bmatrix} = \gamma + f'(z)\gamma^1 \qquad 3(b)$$

2.3. Constitutive relations

In the present paper, the plane stress condition is considered, and the effect of σ_z is neglected. In the, case of FGPs the stress in plane, according to Hook's law, can be written as:

$$\sigma = E(\varepsilon + zk + f(z)k^1 - \varepsilon^{th}) \qquad 4(a)$$

The thermal strain of the EGM plate under temperature condition is:

$$\varepsilon^{th} = \alpha^T(z)\Delta T(z)[1 \quad 1 \quad 0] \qquad 4(b)$$

and the shear stress is:

$$\tau = G(\gamma + f'(z)\gamma^1) \qquad 4(c)$$

where $\sigma = (\sigma_{xx}, \sigma_{yy}, \tau_{xy})^t$, $\tau = (\tau_{yz}, \tau_{xz})^t$, and E and G are defined as:

$$E = \frac{E(z)}{1-\nu^2}\begin{bmatrix}1 & \nu & 0\\ \nu & 1 & 0\\ 0 & 0 & (1-\nu)/2\end{bmatrix} \qquad 4(d)$$

$$G = \frac{E(z)}{2(1+\nu)}\begin{bmatrix}1 & 0\\ 0 & 1\end{bmatrix} \qquad 4(e)$$

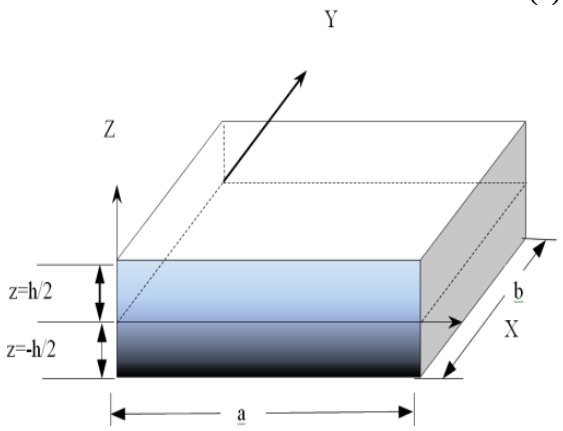

Fig. 1. Representation of exponentially graded rectangular plate.

2.4. Equations of motion

In analytical form, Hamilton's principle is:

$$\int_0^t \delta U + \delta V = 0 \quad 5(a)$$

$$\delta U = \int_A \left\{ \int_{-h/2}^{h/2} \begin{bmatrix} \sigma_x \delta\varepsilon_{xx} + \sigma_y \delta\varepsilon_{yy} \\ + \tau_{xy}\, \delta\gamma_{xy} \\ + \tau_{xz}\delta\gamma_{xz} + \tau_{yz}\delta\gamma_{yz} \end{bmatrix} dz \right\} dx\, dy \quad 5(b)$$

$$\delta V = -\int q\, w\, dx\, dy \quad 5(c)$$

By the substitution of δU and δV in in Eq. 5(a) and integrating by parts and grouping the coefficients of $\delta u_o, \delta v_o, \delta w, \delta\psi_x$, and $\delta\psi_y$, the following equations are obtained:

$$\delta u_0 : N_{x,x} + N_{xy,y} = 0 \quad (6a)$$

$$\delta v_0 : N_{y,y} + N_{xy,x} = 0 \quad (6b)$$

$$\delta w_0 : M_{x,xx} + M_{y,yy} + 2M_{xy,xy} + q = 0 \quad 6(c)$$

$$\delta\theta_x : f^* M_{x,x} + f^* M_{xy,y} + P_{x,x} + P_{xy,y} - f^* Q_{xz} - R_{xz} = 0 \quad (6d)$$

$$\delta\theta_y : f^* M_{y,y} + f^* M_{xy,x} + P_{y,y} + P_{xy,x} - f^* Q_{yz} - R_{yz} = 0 \quad (6e)$$

where the in-plane force and transverse force moment resultants are defined as:

$$\begin{bmatrix} N_x & M_x & P_x \\ N_y & M_y & P_y \\ N_{xy} & M_{xy} & P_{xy} \end{bmatrix} = \int_{-h/2}^{h/2} \begin{bmatrix} \sigma_x \\ \sigma_y \\ \tau_{xy} \end{bmatrix} [1, z, f(z)]\, dz \quad 7(a)$$

$$\begin{bmatrix} Q_{xz} & R_{xz} \\ Q_{yz} & R_{yz} \end{bmatrix} = \int_{-h/2}^{h/2} \begin{bmatrix} \tau_{xz} \\ \tau_{yz} \end{bmatrix} [1, f'(z)]\, dz \quad 7(b)$$

Using Eq. 4(a-c) in Eq. 7(a-b), the stress resultants of exponentially graded material plates can be related to the total strains by:

$$\begin{bmatrix} N \\ M \\ P \end{bmatrix} = \begin{bmatrix} A & B & E \\ B & D & F \\ E & F & H \end{bmatrix} \begin{bmatrix} \varepsilon \\ k \\ k^1 \end{bmatrix} - \begin{bmatrix} N^T \\ M^T \\ P^T \end{bmatrix} \quad 8(a)$$

$$\begin{bmatrix} Q \\ R \end{bmatrix} = \begin{bmatrix} J & K \\ L & M \end{bmatrix} \begin{bmatrix} \gamma \\ \gamma^1 \end{bmatrix} \quad 8(b)$$

where N=[N_x, N_y, N_{xy}]t, M= [M_x, M_y, M_{xy}]^t, P= [P_x, P_y, P_{xy}]^t, Q=[Q_{yz}, Q_{xz}] t , R=[R_{xz}, R_{yz}]^t, NT=[NT_x, NT_y, 0]^t, M= [MT_x, MT_y, 0]^t, and P= [PT_x, PT_y, 0]^t (8c)

$$A = \begin{bmatrix} A_{11} & A_{12} & 0 \\ A_{12} & A_{11} & 0 \\ 0 & 0 & A_{33} \end{bmatrix}; \quad 9(a)$$

$$B = \begin{bmatrix} B_{11} & B_{12} & 0 \\ B_{12} & B_{11} & 0 \\ 0 & 0 & B_{33} \end{bmatrix}; \quad 9(b)$$

$$E = \begin{bmatrix} E_{11} & E_{12} & 0 \\ E_{12} & E_{11} & 0 \\ 0 & 0 & E_{33} \end{bmatrix}; \quad 9(c)$$

$$D = \begin{bmatrix} D_{11} & D_{12} & 0 \\ D_{12} & D_{11} & 0 \\ 0 & 0 & D_{33} \end{bmatrix}; \quad 9(d)$$

$$F = \begin{bmatrix} F_{11} & F_{12} & 0 \\ F_{12} & F_{11} & 0 \\ 0 & 0 & F_{33} \end{bmatrix}; \quad (9e)$$

$$H = \begin{bmatrix} H_{11} & H_{12} & 0 \\ H_{12} & H_{11} & 0 \\ 0 & 0 & H_{33} \end{bmatrix}; \quad 9(f)$$

$$J = \begin{bmatrix} J_{11} & 0 \\ 0 & J_{11} \end{bmatrix}; \quad 9(g)$$

$$K = \begin{bmatrix} K_{11} & 0 \\ 0 & K_{11} \end{bmatrix}; \quad 9(h)$$

$$L = \begin{bmatrix} L_{11} & 0 \\ 0 & L_{11} \end{bmatrix}; \quad 9(i)$$

$$M=\begin{bmatrix} M_{11} & 0 \\ 0 & M_{11} \end{bmatrix}; \qquad 9(j)$$

$$\begin{bmatrix} A_{11} & B_{11} & D_{11} & E_{11} & H_{11} & F_{11} \\ A_{12} & B_{12} & D_{12} & E_{12} & H_{12} & F_{12} \\ A_{33} & B_{33} & D_{33} & E_{33} & H_{33} & F_{33} \end{bmatrix}$$

$$= \int_{-h/2}^{h/2} \frac{E(z)}{1-\nu^2}\left(1, z, z^2, f(z), [f(z)]^2, zf(z)\right)\times \begin{Bmatrix} 1 \\ \nu \\ \frac{1-\nu}{2} \end{Bmatrix} dz \qquad 10(a)$$

$$\begin{bmatrix} J_{11} & K_{11} & M_{11} \end{bmatrix} = \int_{-h/2}^{h/2} \frac{E(z)}{2(1+\nu)}\left(1,\ f'(z), [f'(z)]^2\right) dz \qquad 10(b)$$

$$\begin{bmatrix} N_{xx}^T & M_{xx}^T & P_{xx}^T \\ N_{yy}^T & M_{yy}^T & P_{yy}^T \end{bmatrix} = \int_{-h/2}^{h/2} \frac{E(z)}{1-\nu^2}\begin{bmatrix} 1 & \nu \\ \nu & 1 \end{bmatrix} \alpha^T(z)\Delta T(z)\begin{bmatrix} 1 & z & f(z) \end{bmatrix} dz \qquad 10(c)$$

By substituting Eq. 8(a-b) into Eq. 6(a-e), the displacements expressed as:

$$\begin{aligned} \delta u_0 :& A_{11}u_{0,xx} + A_{12}v_{0,xy} + B_{11}(f^*\psi_{x,xx} - w_{,xxx}) \\ &+ B_{12}(f^*\psi_{y,xy} - w_{,xyy}) + E_{11}\psi_{x,xx} + E_{12}\psi_{y,xy} \\ &+ A_{33}(v_{0,xy} + u_{0,yy}) + B_{33}(f^*\psi_{x,yy} + f^*\psi_{y,xy} \\ &- 2w_{0,xyy}) + E_{33}(\psi_{y,xy} + \psi_{x,yy}) - N_{xx,x}^T \end{aligned} \qquad 11(a)$$

$$\begin{aligned} \delta v_0 :& A_{12}u_{0,xy} + A_{11}v_{0,yy} + B_{12}(f^*\psi_{x,xy} - w_{,xxy}) \\ &+ B_{11}(f^*\psi_{y,yy} - w_{,yyy}) + E_{12}\psi_{x,xy} + E_{11}\psi_{y,yy} \\ &+ A_{33}(v_{0,xx} + u_{0,xy}) + B_{33}(f^*\psi_{x,xy} \\ &+ f^*\psi_{y,xx} - 2w_{0,xxy}) + E_{33}(\psi_{y,xx} + \psi_{x,xy}) - N_{yy,y}^T \end{aligned} \qquad 11(b)$$

$$\begin{aligned} \delta w :& B_{11}(u_{0,xxx} + v_{0,yyy}) + B_{12}(v_{0,xxy} + u_{0,xyy}) \\ &+ D_{11}(f^*\psi_{x,xxx} + f^*\psi_{y,yyy} - w_{,yyyy} - w_{,xxxx}) \\ &+ F_{11}(\psi_{x,xxx} + \psi_{y,yyy}) + F_{12}(\psi_{y,xxy} + \psi_{x,xyy}) \\ &+ D_{12}(f^*\psi_{y,xxy} + f^*\psi_{x,xyy} - 2w_{,xxyy}) \\ &+ 2B_{33}(v_{0,xxy} + u_{0,xyy}) + 2D_{33}(f^*\psi_{x,xyy} \\ &+ f^*\psi_{y,xxy} - 2w_{,xxyy}) + F_{33}(\psi_{x,xyy} + \psi_{y,xxy}) \\ &+ q - N_{xx,xx}^T - N_{yy,yy}^T \end{aligned} \qquad 11(c)$$

$$\begin{aligned} \delta\psi_x :& B_{11}f^*u_{0,xx} + B_{12}f^*v_{0,xy} \\ &+ D_{11}(f^{*2}\psi_{x,xx} - f^*w_{,xxx}) \\ &+ D_{12}(f^{*2}\psi_{y,xy} - f^*w_{,xyy}) + F_{11}f^*\psi_{x,xx} \\ &+ F_{12}f^*\psi_{y,xy} + B_{33}f^*(v_{0,xy} + u_{0,yy}) \\ &+ D_{33}(f^{*2}\psi_{x,yy} + f^{*2}\psi_{y,xy} - 2f^*w_{,xyy}) \\ &+ F_{33}f^*(\psi_{x,yy} + \psi_{y,xy}) \\ &+ E_{11}(u_{0,xx} + v_{0,xy}) + F_{11}(f^*\psi_{x,xx} - w_{,xxx}) \\ &+ F_{12}(f^*\psi_{y,xy} - w_{,xyy}) + H_{11}\psi_{x,xx} + H_{12}\psi_{y,xy} \\ &+ E_{33}(u_{0,yy} + v_{0,xy}) + F_{33}(f^*\psi_{x,yy} + \psi_{y,xy} \\ &- 2w_{0,xyy}) + H_{33}(\theta_{x,yy} + \theta_{y,xy}) \\ &- (J_{11}f^{*2} - K_{11}f^* - L_{11}f^* - M_{11})\theta_x \\ &- f^*M_{xx,x}^T - P_{xx,x}^T \end{aligned} \qquad 11(d)$$

$$\begin{aligned} \delta\psi_y :& B_{12}f^*u_{0,xy} + B_{11}f^*v_{0,yy} \\ &+ D_{12}(f^{*2}\psi_{x,xy} - f^*w_{,xxy}) + D_{11}(f^{*2}\psi_{y,yy} - f^*w_{,yyy}) \\ &+ F_{12}f^*\psi_{x,xy} + F_{11}f^*\psi_{y,yy} + B_{33}f^*(v_{0,xx} + u_{0,xy}) \\ &+ D_{33}(f^{*2}\psi_{x,xy} + f^{*2}\psi_{y,xx} - 2f^*w_{,xxy}) \\ &+ F_{33}f^*(\psi_{x,xy} + \psi_{y,xx}) \\ &+ E_{12}(u_{0,xy} + v_{0,yy}) + F_{12}(f^*\psi_{x,xy} - w_{,xxy}) \\ &+ F_{11}(f^*\psi_{y,yy} - w_{,yyy}) + H_{12}\psi_{x,xy} + H_{11}\psi_{y,yy} \\ &+ E_{33}(u_{0,xy} + v_{0,xx}) + F_{33}(f^*\psi_{x,xy} + \psi_{y,xx} - 2w_{,xxy}) \\ &+ H_{33}(\psi_{x,xy} + \psi_{y,xx}) \\ &- (J_{11}f^{*2} - K_{11}f^* - L_{11}f^* - M_{11})\psi_y \\ &- f^*M_{yy,y}^T - P_{yy,y}^T \end{aligned} \qquad 11(e)$$

In Eq. 3(a), 6(a-e), and 7(a-e) comma (,) represents the partial differentiation w. r. t to the respective coordinate subscripts.

3. Analysis of EGPs

The solutions of Eq. 11(a-e) for EGPs with all sides are simple support, and the boundary conditions for the plate are:

At x=0, a,; $N_{xx}= M_{xx}= P_{xx}= v_0= w_0= \theta_y= \theta_z=0$ 12(a)

At y=0, b; $N_{yy}= M_{yy}= P_{yy}= u_0= w_0= \theta_x= \theta_z=0$ 12(b)

The sinusoidal variation of mechanical and thermal load is chosen as:

$$q(x,y) = q\sin\alpha x \sin\beta y \quad (13a)$$

The load ($q(x,y)$) is in the thickness direction and q is the intensity of the load:

$$T(x,y,z) = [T_1(x,y) + \frac{z}{h}T_2(x,y) + \frac{1}{h}[zf^* + f(z)]T_3(x,y)]\sin\alpha x \sin\beta y \quad 13(b)$$

Solution expressions that totally satisfy the above conditions in Eq. (14) are:

$$u_0(x,y) = u\cos\alpha x \sin\beta y \quad 14(a)$$

$$v_0(x,y,t) = v\sin\alpha x \cos\beta y \quad 14(b)$$

$$w(x,y) = w\sin\alpha x \sin\beta y \quad 14(c)$$

$$\psi_x(x,y) = \psi\cos\alpha x \sin\beta y \quad 14(d)$$

$$\psi_y(x,y) = \zeta\sin\alpha x \cos\beta y \quad 14(e)$$

where, 0≤x≤a; 0≤y≤b, $\alpha = \pi/a$ and $\beta = \pi/b$.
By substituting Eq. 14(a-e) into equations of motion given by Eq. 11(a-e), and by simplifying these expressions leads to a set of 5 algebraic equations involving *u*, *v*, *w*, ψ, and ζ and solved using an inverse method. These algebraic expressions arranged in matrix form:

$$[\text{STIFFNESS MATRIX}]_{5\times5}[\text{UNKNOWNS}]_{5\times1} = [\text{FORCE MATRIX}]_{5\times1}. \quad (15)$$

The elements of the stiffness matrix are given in the Appendix.
Unknowns of the above equations gives *u*, *v*, *w*, ψ, and ζ are used to compute u_o, v_o, w_o, ψ_x, and ψ_y.

4. Results and discussion

The proposed displacement field dependent on '*r*', which is calculated to provide deflections and stresses of EGPs close to the three-dimensional solutions [23]. It is noticed that the present novel theory estimates the bending results with minimum error with three-dimensional solutions [35] at *r*=4.21. The bending results of simply supported EGPs using proposed HSDT for deflections and stresses under mechanical and thermal loads are presented. These numerical results are compared with the three-dimensional solutions, the well-known TPT, and HSDT, given by Zenkour [23] and Mantari et al. [24, 25].
In the present study, the displacements and normal and shear stresses, are found at their maximum absolute values. The *u* and τ_{xz} are evaluated at (0, b/2), while *v* and transverse shear stress τ_{yz} are evaluated at (a/2, 0) and τ_{xy} is evaluated at (0, 0). The normal stresses $\bar{\sigma}_{yy}$ and *w* is evaluated at (a/2, b/2).
All the results are given in the non-dimensional quantities as follows:

$$\bar{u}, \bar{v}, \bar{w} = \frac{10}{\frac{qa^4}{E_m h^3} + \frac{10\alpha_m T_2 a^2}{h}}(u, v, w) \quad 16(a)$$

$$\bar{\sigma}_{xx}, \bar{\sigma}_{yy} = \frac{1}{\frac{qa^2}{h^2} + \frac{E_m\alpha_m T_2 a^2}{h^2}}(\sigma_{xx}, \sigma_{yy}) \quad 16(b)$$

$$\bar{\tau}_{xz}, \bar{\tau}_{yz} = \frac{1}{\frac{qa}{h} + \frac{E_m\alpha_m T_2 a}{h}}(\tau_{xz}, \tau_{yz}) \quad 16(c)$$

$$\bar{\tau}_{xy} = \frac{10}{\frac{qa^2}{h^2} + \frac{10E_m\alpha_m T_2 a^2}{h^2}}\tau_{xy} \quad 16(d)$$

The numerical results of the present HSDT are presented for various (*b/a*) ratios and *p*. Fig. 2 shows the variation of the exponential function in the thickness of an EGP and varies according to the Eq. (17).

$$Exp\left[p\left(\frac{z}{h} + \frac{1}{2}\right)\right] \quad (17)$$

Tables 1-3 present results of dimensionless center deflections, a/h = 2, 4, 10, respectively, subjected to mechanical load.

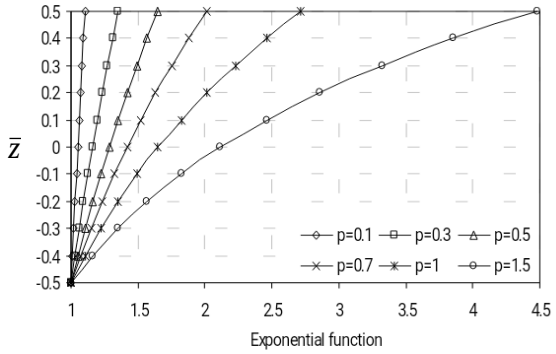

Fig. 2. Distribution of exponential function through the thickness of EGP.

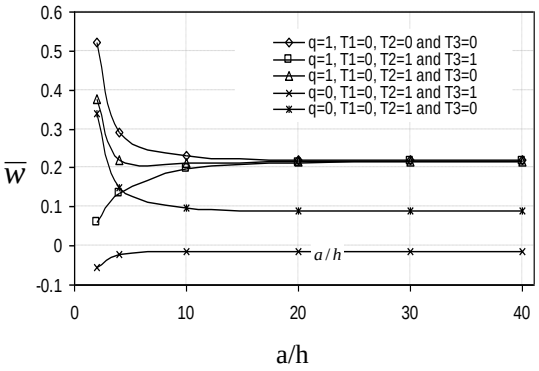

Fig. 3(a). Influence of thermomechanical loads on $\bar{w}$ of square EGM Plate (p=0.5) vs. a/h.

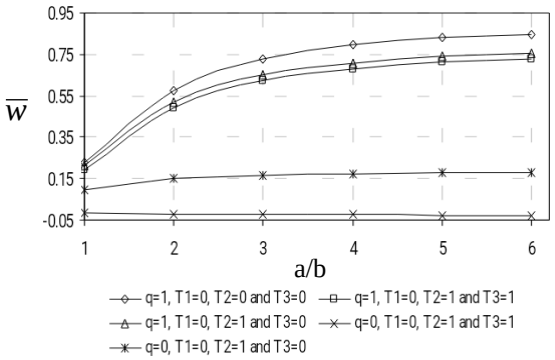

Fig. 3(b). Infuence of thermo mechanical loads on $\bar{w}$ of EGP (p=0.5, a/h=10) vs. a/b.

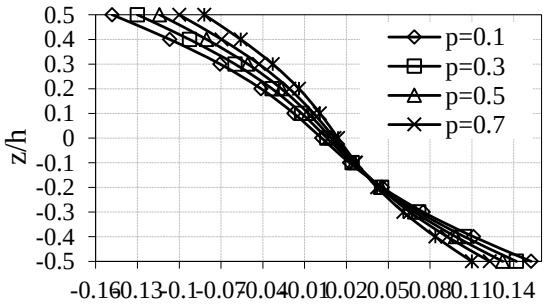

Fig. 4(a). Influence of $\bar{u}$ on (a/h=2) rectangular plate (b/a=6).

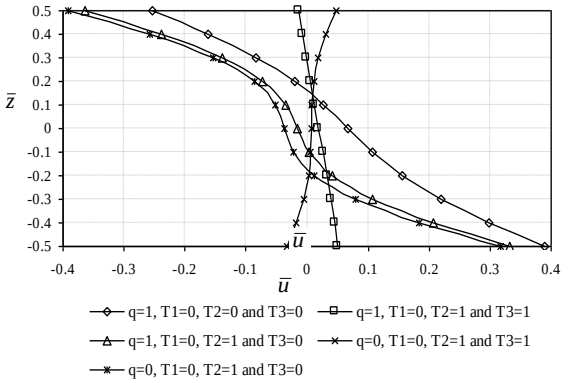

Fig. 4(b). Influence of $\bar{v}$ on (a/h=2) rectangular (b/a=6) plate.

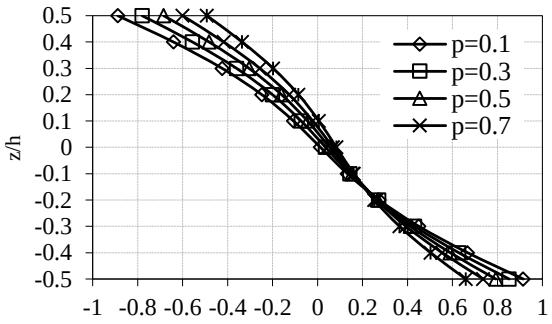

Fig. 4(c). Influence of thermo mechanical loads on $\bar{u}$ of rectangular (b/a=2) EGP (p=1.5, a/h=2).

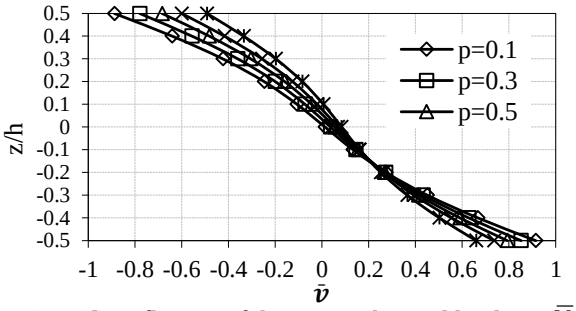

Fig. 4(d). Influence of thermomechanical loads on $\bar{v}$, on rectangular (b/a=2) EGP (p=1.5, a/h=2).

The present results without inclusion of the thickness stretching effect, $\varepsilon_{zz} = 0$ are agreed well to three dimensional solutions and the solutions given by Mantari and Guedes Soares [25] who considered $\varepsilon_{zz} \neq 0$. The present theory results slightly under-estimates the 3D solutions for larger values of (*b/a*) and slightly over-estimates for smaller values of (*b/a*). Mantari and Guedes Soares [25], also gave over-estimated center deflections in which the thickness stretching influence was not included. However, TPT [23] and HPT [23] provide

under-estimated center deflections even the thickness stretching included. Therefore, the present theory is more accurate in estimating the center plate deflections. The dimensionless center deflections decrease with increasing *p* and decreasing b/a. This is due to the fact that the Young's modulus of the EGM plate increases.

Fig. 3(a) shows the influence of a/h on the dimensionless center deflection of EGP (p=0.5). The influence of thermal and mechanical loads is considered. The deflection is more for plate exposed to mechanical load only, while it decreases with the inclusion of thermal load (T2). The deflection behavior of the plate is quite different and increases when the thermal load (T3) is included. Also, it was found that the shear deformation effect decreases for a/h >20. Fig. 3(b) shows the influence of *b/a* on the dimensionless center deflection for EGP (p=0.5). It is noted that, the center deflection increases with the increase in aspect ratio at all loading conditions, except q=0, T1=0, T2=1, and T3=1. Also. It was observed that the inclusion of T2=1 and T3=1 decreases the center plate deflections.

The thickness distributions of in-plane ($\bar{u}, \bar{v}$) displacements for *p*=0.1, 0.3, 0.5, 0.7, and 1 at *a/h*= 2 and *b/a*=6 under mechanical load is shown in Fig. 4(a-b). The in-plane displacements increase from the top side to the bottom side of the plate. At $\bar{z} \cong -0.16$, the in-plane displacements are independent of the exponent, *p*. Fig. 4(c-d) shows the influence of mechanical and thermal loads on in-plane displacements of the EGM plate through the thickness for *p*=1. 5, at *a/h*=2 and *b/a*=2. The in-plane displacements increase from the top side of the plate to the bottom side of the plate due to the mechanical load, *q*=0 or 1, T2=1, and T3=0. However, the opposite can be found when *q*=0 and T2=T3=1. The figures accentuate the pronounced influence took part by the different thermal and bending loads on the analyzed in-plane displacements.

Tables 4 to 6 present results of $\bar{\sigma}_{yy}$ of square and rectangular EGPS, a/h: 2, 4, 10. The results for the $\bar{\sigma}_{yy}$ increase with increasing *p*, while it decreases with b/a. The present theory results slightly under-estimating the normal stresses $\bar{\sigma}_{yy}$ for rectangular plates at a/h:2 and 4, and for square plates at a/h:4, slightly over-estimating. The supremacy of the present novel theory against TPT [23], HPT [23], and Mantari et al. [24] can be noticed.

The $\bar{\sigma}_{yy}$ is compressive at and beneath the mid-plane, and the tensile over the mid-plane for *p*=0.1, 0.3, 0.5, 0.7, and 1 at *a/h*= 4 and *b/a*=2 under mechanical load is shown in Fig. 5 (a). For the various chosen *p*, the plate with *p*=1 gives the maximum tensile stress and compressive stress at the upper side and lower side of the plate, respectively. At $\bar{z} \cong -0.275$, the in-plane compressive stresses and at $\bar{z} \cong 0.31$, the in-plane tensile stresses are independent of exponent, *p*. Fig. 5(b) shows the influence of mechanical and thermal loads on $\bar{\sigma}_{yy}$ of EGM plate through the thickness for *p*=1.5 at *a/h*=2 and *b/a*=2. The figure emphasis, in-plane stresses are greatly influenced by different thermal and mechanical loads.

Table 7 presents the results of $\bar{\sigma}_{xx}$ of square and rectangular EGM plates at *a/h*:10. The results for $\bar{\sigma}_{xx}$, increases with increase in *p* and decreases in *b/a*. The present HSDT results are in very good agreement with those reported by Mantari et al. [24 , 25]. From Fig. 6(a-b) a similar inference can be drawn from the distribution of $\bar{\sigma}_{xx}$. Fig. 7(a) shows the distribution of in-plane shear stress, $\bar{\tau}_{xy}$ along the thickness of the EGPs, a/h= 2, 4 10 for p=0.5 and b/a=2 under mechanical load. The in-plane shear stresses, $\bar{\tau}_{xy}$, are compressive over the middle plane of the plate and tensile at and below the middle plane of the plate.

Note that for different a/h ratios chosen, the very thick plate, a/h=2 yield maximum tensile stress and minimum compressive shear stress at the bottom surface and top surface of the plate, respectively. It is important to observe that, the shear stress varies slightly, as the a/h increases through the thickness direction. At $\bar{z} \cong \pm 0.34$, the $\bar{\tau}_{xy}$ are independent of the thickness of the plate. The distribution of $\bar{\tau}_{xy}$ through the thickness direction of the EGM plate under mechanical and thermal loads is shown in Fig. 7(b). It is noticed that, the stresses are independent of the type of load at $\bar{z} \cong$ 0.17 and 0.21.

Table 1. Comparison of $\overline{w}$ for several EGPs, a/h=2.

b/a	Theory	ε_{zz}	n=0.1	n=0.3	n=0.5	n=0.7	n=1	n=1.5
6	3-D[23]		1.63774	1.48846	1.35184	1.22688	1.05929	0.82606
	Present	**0**	**1.63783**	**1.48131**	**1.33916**	**1.21009**	**1.03853**	**0.802941**
	Mantari et al.[25]	≠0	1.63654	1.47953	1.33644	1.20618	1.03325	0.79387
	Manteri et al.[24]	0	1.73465	1.56884	1.41822	1.28145	1.10032	0.84996
	TPT [23]	≠0	1.62939	1.47309	1.33066	1.20101	1.02823	0.79056
	HPT [23]	≠0	1.54777	1.39964	1.26493	1.14249	0.97956	0.7556
5	3-D[23]		1.60646	1.46007	1.32607	1.20349	1.03907	0.81024
	Present	**0**	**1.61009**	**1.45623**	**1.31649**	**1.18962**	**1.02097**	**0.789399**
	Mantari et al.[25]	≠0	1.60532	1.4513	1.31094	1.18315	1.01352	0.77867
	Manteri et al.[24]	0	1.70246	1.53972	1.39188	1.25762	1.07981	0.83401
	TPT [23]	≠0	1.59825	1.44493	1.30522	1.17804	1.00856	0.7754
	HPT [23]	≠0	1.51991	1.37444	1.24214	1.12188	0.96184	0.74184
4	3-D[23]		1.55146	1.41013	1.28074	1.16235	1.00352	0.78241
	Present	**0**	**1.5611**	**1.41193**	**1.27645**	**1.15345**	**0.989959**	**0.765472**
	Mantari et al.[25]	≠0	1.55042	1.40166	1.2661	1.14267	0.97884	0.75195
	Manteri et al.[24]	0	1.64584	1.48849	1.34553	1.21569	1.04374	0.80596
	TPT [23]	≠0	1.54348	1.39541	1.26048	1.13764	0.97395	0.74874
	HPT [23]	≠0	1.47089	1.33009	1.20201	1.08559	0.93065	0.71762
3	3-D[23]		1.44295	1.3116	1.19129	1.08117	0.93337	0.7275
	Present	**0**	**1.46363**	**1.32378**	**1.19677**	**1.08147**	**0.928233**	**0.717834**
	Mantari et al.[25]	≠0	1.4421	1.30373	1.17761	1.06279	0.91041	0.69925
	Manteri et al.[24]	0	1.53405	1.38735	1.25402	1.13291	0.97254	0.7506
	TPT [23]	≠0	1.43542	1.29771	1.17221	1.05795	0.90567	0.69615
	HPT [23]	≠0	1.37394	1.24238	1.2269	1.01386	0.86898	0.66977
2	3-D[23]		1.19445	1.08593	0.9864	0.8952	0.77266	0.60174
	Present	**0**	**1.23607**	**1.11797**	**1.01074**	**0.913395**	**0.784033**	**0.606451**
	Mantari et al.[25]	≠0	1.19408	1.07949	0.97503	0.8799	0.75377	0.57862
	Manteri et al.[24]	0	1.2776	1.15533	1.04413	0.94307	0.80929	0.62377
	TPT [23]	≠0	1.18798	1.07399	0.97009	0.87548	0.74936	0.57578
	HPT [23]	≠0	1.1508	1.04052	0.94012	0.84878	0.72712	0.55975
1	3-D[23]		0.57693	0.52473	0.47664	0.4324	0.37269	0.28904
	Present	**0**	**0.63847**	**0.577441**	**0.522**	**0.47166**	**0.404741**	**0.312871**
	Mantari et al.[25]	≠0	0.57789	0.5224	0.47179	0.42567	0.36485	0.27939
	Manteri et al.[24]	0	0.63625	0.57517	0.51948	0.46874	0.40178	0.30791
	TPT [23]	≠0	0.57308	0.51806	0.46788	0.42216	0.36117	0.27712
	HPT [23]	≠0	0.58586	0.52955	0.47814	0.43127	0.36871	0.28246

Table 2. Comparison of $\overline{w}$ for several EGPs, a/h=4.

b/a	Theory	ε_{zz}	n=0.1	n=0.3	n=0.5	n=0.7	n=1	n=1.5
6	3-D[23]		1.1714	1.06218	0.96331	0.87378	0.75501	0.59193
	Present	**0**	**1.16801**	**1.05715**	**0.95706**	**0.86666**	**0.74712**	**0.58377**
	Mantari et al.[25]	≠0	1.17033	1.05825	0.95628	0.86359	0.74032	0.57128
	Manteri et al.[24]	0	1.19202	1.07885	0.97667	0.88437	0.76228	0.59545
	TPT [23]	≠0	1.16681	1.05509	0.95345	0.86107	0.73821	0.56969
	HPT [23]	≠0	1.00649	0.91087	0.82448	0.7464	0.64306	0.50178
5	3-D[23]		1.14589	1.03906	0.94236	0.85478	0.73859	0.57904
	Present	**0**	**1.14315**	**1.03465**	**0.93668**	**0.84821**	**0.73120**	**0.57133**
	Mantari et al.[25]	≠0	1.14484	1.0352	0.93545	0.84478	0.72419	0.55882
	Manteri et al.[24]	0	1.16628	1.05555	0.95557	0.86525	0.74578	0.58253
	TPT [23]	≠0	1.1414	1.0321	0.93268	0.84231	0.72212	0.55726
	HPT [23]	≠0	0.98508	0.8915	0.80694	0.7305	0.62935	0.49105
4	3-D[23]		1.10115	0.99852	0.9056	0.82145	0.70979	0.55643
	Present	**0**	**1.0995**	**0.99513**	**0.90091**	**0.81581**	**0.70326**	**0.54948**
	Mantari et al.[25]	≠0	1.10013	0.99477	0.89891	0.81178	0.69589	0.53696
	Manteri et al.[24]	0	1.12113	1.01469	0.91856	0.83172	0.71685	0.55987
	TPT [23]	≠0	1.09682	0.9918	0.89625	0.80941	0.6939	0.53546
	HPT [23]	≠0	0.94753	0.8575	0.77615	0.70262	0.60529	0.47222
3	3-D[23]		1.01338	0.91899	0.8335	0.75606	0.65329	0.51209
	Present	**0**	**1.01369**	**0.91746**	**0.83059**	**0.75212**	**0.64833**	**0.50652**
	Mantari et al.[25]	≠0	1.01243	0.91546	0.82724	0.74704	0.64037	0.49408
	Manteri et al.[24]	0	1.03254	0.9345	0.84594	0.76593	0.66008	0.51541
	TPT [23]	≠0	1.00938	0.91272	0.82479	0.74486	0.63854	0.4927
	HPT [23]	≠0	0.87379	0.79076	0.71571	0.64787	0.55806	0.43525
2	3-D[23]		0.81529	0.73946	0.67075	0.60846	0.52574	0.412
	Present	**0**	**0.819111**	**0.741343**	**0.67111**	**0.60767**	**0.52375**	**0.40908**
	Mantari et al.[25]	≠0	0.81448	0.73647	0.66547	0.60093	0.51508	0.39732
	Manteri et al.[24]	0	0.83246	0.75338	0.68192	0.61734	0.53188	0.41503
	TPT [23]	≠0	0.81202	0.73425	0.6635	0.59917	0.51361	0.3962
	HPT [23]	≠0	0.707	0.63979	0.57901	0.52405	0.45126	0.35169
1	3-D[23]		0.349	0.31677	0.28747	0.26083	0.22534	0.18054
	Present	**0**	**0.35522**	**0.32145**	**0.29091**	**0.26330**	**0.22674**	**0.17674**
	Mantari et al.[25]	≠0	0.3486	0.31519	0.28477	0.2571	0.22028	0.16972
	Manteri et al.[24]	0	0.36017	0.32589	0.29485	0.26676	0.22952	0.17854
	TPT [23]	≠0	0.34749	0.31419	0.28388	0.25631	0.21961	0.16922
	HPT [23]	≠0	0.31111	0.28146	0.25461	0.23027	0.198	0.15377

Table 3. Comparison of $\overline{w}$ for several EGPs, a/h=10.

b/a	Theory	ε_z	n=0.1	n=0.3	n=0.5	n=0.7	n=1.0	n=1.5	n=2.0	n=2.5	n=3.0
6	**Present**	**0**	**1.035**	**0.9370**	**0.8488**	**0.7694**	**0.6645**	**0.5216**	**0.4101**	**0.3223**	**0.2530**
	Mantari et al.[25]	$\neq 0$	1.0354	0.9363	0.8462	0.7644	0.6558	0.5063	0.3913	0.3018	0.2324
	Manteri et al.[24]	0	1.0388	0.9405	0.852	0.7723	0.667	0.5236	0.4115	0.3235	0.2539
	TPT [23]	$\neq 0$	1.0321	0.9333	0.8436	0.7621	0.6538	0.5054	0.3901	0.3006	0.2314
5	**Present**	**0**	**1.0112**	**0.9155**	**0.8293**	**0.7517**	**0.6493**	**0.5096**	**0.4006**	**0.3149**	**0.2471**
	Mantari et al.[25]	$\neq 0$	1.0115	0.9147	0.8267	0.7468	0.6406	0.4952	0.3823	0.2948	0.2271
	Manteri et al.[24]	0	10.149	0.9189	0.8324	0.7545	0.6516	0.5115	0.402	0.316	0.248
	TPT [23]	$\neq 0$	1.0083	0.9118	0.8241	0.7445	0.6387	0.4938	0.381	0.2937	0.2261
4	**Present**	**0**	**0.9694**	**0.8777**	**0.7951**	**0.7207**	**0.6225**	**0.4886**	**0.3841**	**0.3019**	**0.2369**
	Mantari et al.[25]	$\neq 0$	0.9696	0.8768	0.7925	0.7159	0.6141	0.4747	0.3664	0.2826	0.2177
	Manteri et al.[24]	0	0.973	0.8809	0.798	0.7233	0.6247	0.4903	0.3854	0.3029	0.2377
	TPT [23]	$\neq 0$	0.9665	0.8741	0.79	0.7137	0.6123	0.4733	0.3653	0.2815	0.2167
3	**Present**	**0**	**0.8878**	**0.8037**	**0.7281**	**0.6599**	**0.5700**	**0.4474**	**0.3517**	**0.2765**	**0.21699**
	Mantari et al.[25]	$\neq 0$	0.8877	0.8027	0.7255	0.6554	0.5622	0.4346	0.3355	0.2587	0.1992
	Manteri et al.[24]	0	0.8909	0.8066	0.7307	0.6622	0.572	0.4489	0.3528	0.2773	0.2176
	TPT [23]	$\neq 0$	0.8849	0.8002	0.7233	0.6534	0.5605	0.4333	0.3344	0.2577	0.1983
2	**Present**	**0**	**0.7043**	**0.6376**	**0.5776**	**0.5235**	**0.4522**	**0.3549**	**0.2789**	**0.2192**	**0.1720**
	Mantari et al.[25]	$\neq 0$	0.7037	0.6364	0.5752	0.5196	0.4457	0.3445	0.2659	0.205	0.1579
	Manteri et al.[24]	0	0.7066	0.6397	0.5795	0.5252	0.4536	0.356	0.2797	0.2198	0.1724
	TPT [23]	$\neq 0$	0.7015	0.6344	0.5734	0.518	0.4444	0.3435	0.2651	0.2043	0.1572
1	**Present**	**0**	**0.2806**	**0.2540**	**0.2301**	**0.2085**	**0.1800**	**0.1412**	**0.1109**	**0.0871**	**0.0683**
	Mantari et al.[25]	$\neq 0$	0.2799	0.2531	0.2287	0.2066	0.1772	0.137	0.1057	0.0814	0.0627
	Manteri et al.[24]	0	0.2816	0.255	0.2309	0.2093	0.1807	0.1417	0.1112	0.0873	0.0684
	TPT [23]	$\neq 0$	0.279	0.2523	0.228	0.206	0.1767	0.1366	0.1053	0.0811	0.0624

The $\overline{\sigma}_{xz}$ in different EG rectangular plates, p= 0.1, 0.3, 0.5, 0.7, 1, 1.5, 2, 2.5, and 3 for a/h=10 is presented in Table 8. From this table, it is observed that the stress, $\overline{\sigma}_{xz}$ decreases with both the increase in the exponent, p, and the decrease in the aspect ratio, b/a. The present stress results are very close to those of Manteri et al. [24, 25], but TPT [23] over-estimating the stresses. Fig. 8(a) shows the distribution of shear stresses $\overline{\sigma}_{xz}$, through the thickness of square EGPs, p= {0.1, 0.3, 0.5, 0.7, 1}, for a/h=10.

From Fig. 8(a), it can be noticed that the stresses are maximum at the mid-plane and zero at the upper side and lower side of the plate. The stresses decrease with the increase in the exponent, p, below the mid-plane and increases at and above the mid-plane. The effect of aspect ratio on stress, $\overline{\sigma}_{yz}$ distributions along the thickness of the EGP for a/h: 2 at p=0.5 is shown in Fig 8(b). The stresses are zero at the lower side and upper side of the plate and maximum at the mid-plane. The stresses decrease with the increase in b/a.

Table 4. Comparison of $\overline{\sigma}_{yy}$ for EGPs, a/h=2.

b/a	Theory	ε_{zz}	n=0.1	n=0.3	n=0.5	n=0.7	n=1	n=1.5
6	3-D[23]	≠0	0.29429	0.31008	0.32699	0.34508	0.37456	0.43051
	Present	**0**	**0.22421**	**0.24048**	**0.25775**	**0.27608**	**0.30568**	**0.36116**
	Mantari et al.[25]	≠0	0.27628	0.29544	0.31592	0.3378	0.37374	0.44163
	Manteri et al.[24]	0	0.21871	0.23447	0.25122	0.269	0.29804	0.34981
	TPT [23]	≠0	0.29119	0.31184	0.33385	0.35731	0.39547	0.46786
	HPT [23]	≠0	0.31192	0.33462	0.35873	0.38433	0.42573	0.50345
5	3-D[23]	≠0	0.29674	0.31277	0.32993	0.34829	0.37821	0.435
	Present	**0**	**0.22808**	**0.24464**	**0.26223**	**0.28089**	**0.31105**	**0.36759**
	Mantari et al.[25]	≠0	0.27892	0.29833	0.31905	0.34119	0.37755	0.44614
	Manteri et al.[24]	0	0.22185	0.23784	0.25484	0.27288	0.30236	0.35485
	TPT [23]	≠0	0.29353	0.31439	0.33662	0.36032	0.39884	0.47187
	HPT [23]	≠0	0.31327	0.33607	0.3603	0.38604	0.42764	0.50573
4	3-D[23]	≠0	0.30084	0.31727	0.33486	0.35368	0.38435	0.44257
	Present	**0**	**0.23473**	**0.2518**	**0.26993**	**0.28918**	**0.32029**	**0.37868**
	Mantari et al.[25]	≠0	0.28335	0.30317	0.32431	0.3469	0.38394	0.45373
	Manteri et al.[24]	0	0.22715	0.24354	0.26096	0.27945	0.30968	0.36337
	TPT [23]	≠0	0.29743	0.31864	0.34124	0.36533	0.40446	0.47857
	HPT [23]	≠0	0.31543	0.33842	0.36285	0.38878	0.43072	0.50943
3	3-D[23]	≠0	0.30808	0.32525	0.34362	0.36329	0.39534	0.45619
	Present	**0**	**0.24721**	**0.26524**	**0.28441**	**0.30477**	**0.33772**	**0.39965**
	Mantari et al.[25]	≠0	0.29122	0.31177	0.33369	0.35707	0.39537	0.46732
	Manteri et al.[24]	0	0.23675	0.25387	0.27206	0.29138	0.32297	0.37881
	TPT [23]	≠0	0.30421	0.32606	0.34933	0.3741	0.41432	0.49035
	HPT [23]	≠0	0.3189	0.3422	0.36695	0.39323	0.43572	0.51545
2	3-D[23]	≠0	0.31998	0.33849	0.35833	0.37956	0.41417	0.47989
	Present	**0**	**0.27199**	**0.29198**	**0.31327**	**0.33594**	**0.37270**	**0.44207**
	Mantari et al.[25]	≠0	0.30422	0.32613	0.34945	0.37427	0.41483	0.49052
	Manteri et al.[24]	0	0.25385	0.27231	0.29193	0.31276	0.3469	0.40636
	TPT [23]	≠0	0.31463	0.33758	0.362	0.38796	0.43003	0.50925
	HPT [23]	≠0	0.32223	0.34592	0.37109	0.39782	0.44102	0.52203
1	3-D[23]	≠0	0.31032	0.32923	0.34953	0.37127	0.40675	0.47405
	Present	**0**	**0.29301**	**0.31530**	**0.33915**	**0.36467**	**0.40634**	**0.48585**
	Mantari et al.[25]	≠0	0.29244	0.31468	0.33826	0.36325	0.40405	0.47848
	Manteri et al.[24]	0	0.25215	0.271	0.29102	0.31227	0.34773	0.40347
	TPT [23]	≠0	0.29554	0.31811	0.34208	0.3675	0.40851	0.48508
	HPT [23]	≠0	0.28882	0.31072	0.33398	0.35866	0.39852	0.47305

Table 5. Comparison of $\overline{\sigma}_{yy}$ for EGPs, a/h=4.

b/a	Theory	ε_{zz}	n=0.1	n=0.3	n=0.5	n=0.7	n=1	n=1.5
6	3-D[23]	≠0	0.21814	0.23211	0.24699	0.26284	0.28857	0.33725
	Present	**0**	**0.20242**	**0.21652**	**0.23149**	**0.24740**	**0.27315**	**0.32165**
	Mantari et al.[25]	≠0	0.21265	0.22547	0.23934	0.2544	0.27953	0.32937
	Manteri et al.[24]	0	0.20097	0.21493	0.22976	0.24553	0.27105	0.31917
	TPT [23]	≠0	0.23686	0.25204	0.2683	0.28574	0.31441	0.3699
	HPT [23]	≠0	0.2817	0.30133	0.32219	0.34435	0.38024	0.44786
5	3-D[23]	≠0	0.2206	0.23476	0.24984	0.26591	0.29199	0.34133
	Present	**0**	**0.20529**	**0.21959**	**0.23478**	**0.25092**	**0.27705**	**0.32626**
	Mantari et al.[25]	≠0	0.21524	0.2283	0.24241	0.25772	0.28323	0.33373
	Manteri et al.[24]	0	0.20366	0.21781	0.23285	0.24883	0.2747	0.32346
	TPT [23]	≠0	0.23912	0.2545	0.27097	0.28863	0.31764	0.37371
	HPT [23]	≠0	0.28261	0.30231	0.32323	0.34547	0.38148	0.44934
4	3-D[23]	≠0	0.2247	0.23918	0.2546	0.27103	0.2977	0.34816
	Present	**0**	**0.21012**	**0.22476**	**0.24032**	**0.25685**	**0.28361**	**0.33402**
	Mantari et al.[25]	≠0	0.21957	0.23302	0.24754	0.26327	0.28943	0.34105
	Manteri et al.[24]	0	0.20818	0.22264	0.23802	0.25435	0.28081	0.33066
	TPT [23]	≠0	0.24286	0.25858	0.27539	0.29342	0.32299	0.38004
	HPT [23]	≠0	0.28399	0.30379	0.32483	0.34719	0.38338	0.45159
3	3-D[23]	≠0	0.23188	0.24692	0.26295	0.28002	0.30775	0.36021
	Present	**0**	**0.2188**	**0.23406**	**0.25027**	**0.26751**	**0.29542**	**0.34802**
	Mantari et al.[25]	≠0	0.22721	0.24137	0.25663	0.27312	0.30044	0.35404
	Manteri et al.[24]	0	0.21619	0.23122	0.2472	0.26417	0.29166	0.34346
	TPT [23]	≠0	0.24931	0.26563	0.28307	0.30174	0.3323	0.39106
	HPT [23]	≠0	0.28588	0.30583	0.32702	0.34954	0.38601	0.45471
2	3-D[23]	≠0	0.24314	0.25913	0.27618	0.29434	0.32385	0.37968
	Present	**0**	**0.23376**	**0.25011**	**0.26748**	**0.28596**	**0.31590**	**0.37238**
	Mantari et al.[25]	≠0	0.23953	0.25497	0.27154	0.28936	0.3187	0.37562
	Manteri et al.[24]	0	0.22943	0.24542	0.2624	0.28045	0.30967	0.36473
	TPT [23]	≠0	0.25878	0.27609	0.29456	0.31428	0.34644	0.40788
	HPT [23]	≠0	0.28539	0.30534	0.32655	0.34908	0.38556	0.45428
1	3-D[23]	≠0	0.22472	0.23995	0.25621	0.27356	0.30177	0.35885
	Present	**0**	**0.22527**	**0.24121**	**0.25818**	**0.27625**	**0.30557**	**0.36100**
	Mantari et al.[25]	≠0	0.22372	0.23907	0.25544	0.27291	0.30137	0.35555
	Manteri et al.[24]	0	0.21636	0.23157	0.24774	0.26492	0.29273	0.34508
	TPT [23]	≠0	0.23457	0.25098	0.26842	0.28698	0.31706	0.37386
	HPT [23]	≠0	0.2408	0.25783	0.27593	0.29515	0.32627	0.38482

Table 6. Comparison of $\bar{\sigma}_{yy}$ for EGPs, a/h=10.

b/a	Theory	ε_{zz}	n=0.1	n=0.3	n=0.5	n=0.7	n=1.0	n=1.5	n=2.0	n=2.5	n=3.0
6	**Present**	**0**	**0.1962**	**0.20969**	**0.2240**	**0.2392**	**0.2638**	**0.3103**	**0.3646**	**0.4279**	**0.5017**
	Mantari et al.[25]	≠0	0.1954	0.2065	0.2185	0.2317	0.254	0.2988	0.3552	0.4255	0.5115
	Manteri et al.[24]	0	0.198	0.2094	0.2237	0.2389	0.2635	0.31	0.3642	0.4275	0.5011
	TPT [23]	≠0	0.2223	0.236	0.2507	0.2665	0.2926	0.3435	0.4054	0.4805	0.5708
5	**Present**	**0**	**0.1988**	**0.2124**	**0.2269**	**0.2423**	**0.2673**	**0.3144**	**0.3695**	**0.4336**	**0.5083**
	Mantari et al.[25]	≠0	0.198	0.2093	0.2216	0.235	0.2577	0.3031	0.3602	0.4312	0.5179
	Manteri et al.[24]	0	0.1985	0.2122	0.2267	0.2421	0.267	0.314	0.369	0.4331	0.5077
	TPT [23]	≠0	0.2245	0.2385	0.2534	0.2694	0.2958	0.3473	0.4098	0.4855	0.5764
4	**Present**	**0**	**0.2031**	**0.2171**	**0.2319**	**0.2476**	**0.2732**	**0.3213**	**0.3775**	**0.4431**	**0.5195**
	Mantari et al.[25]	≠0	0.2023	0.214	0.2267	0.2406	0.2638	0.3104	0.3686	0.4407	0.5282
	Manteri et al.[24]	0	0.2028	0.2168	0.2316	0.2473	0.2728	0.3208	0.377	0.4424	0.5187
	TPT [23]	≠0	0.2283	0.2425	0.2578	0.2742	0.3012	0.3535	0.417	0.4937	0.5857
3	**Present**	**0**	**0.2108**	**0.2252**	**0.2406**	**0.2570**	**0.2835**	**0.3335**	**0.3918**	**0.4599**	**0.5392**
	Mantari et al.[25]	≠0	0.2099	0.2224	0.2358	0.2504	0.2748	0.3233	0.3835	0.4575	0.5472
	Manteri et al.[24]	0	0.2104	0.2248	0.2402	0.2565	0.2829	0.3328	0.391	0.4589	0.538
	TPT [23]	≠0	0.2347	0.2495	0.2654	0.2825	0.3104	0.3645	0.4296	0.508	0.6016
2	**Present**	**0**	**0.223**	**0.2385**	**0.2548**	**0.2722**	**0.3002**	**0.3532**	**0.4151**	**0.4873**	**0.5713**
	Mantari et al.[25]	≠0	0.2223	0.236	0.2507	0.2666	0.293	0.3447	0.4079	0.4846	0.5768
	Manteri et al.[24]	0	0.2225	0.2378	0.2541	0.2713	0.2993	0.3521	0.4137	0.4855	0.5692
	TPT [23]	≠0	0.2441	0.2599	0.2768	0.2949	0.3244	0.381	0.4486	0.5291	0.6246
1	**Present**	**0**	**0.2075**	**0.2218**	**0.2370**	**0.2532**	**0.2794**	**0.3288**	**0.3865**	**0.4539**	**0.5324**
	Mantari et al.[25]	≠0	0.2063	0.2199	0.2344	0.2499	0.2753	0.324	0.3819	0.4506	0.5317
	Manteri et al.[24]	0	0.2062	0.2204	0.2355	0.2515	0.2774	0.3264	0.3835	0.4502	0.5278
	TPT [23]	≠0	0.2196	0.2345	0.2503	0.2671	0.2944	0.346	0.4065	0.4775	0.5603

Table 7. Comparison of $\bar{\sigma}_{xx}$ for EGPs, a/h=10.

b/a	Theory	ε_{zz}	n=0.1	n=0.3	n=0.5	n=0.7	n=1.0	n=1.5	n=2.0	n=2.5	n=3.0
6	**Present**	**0**	**0.6036**	**0.6450**	**0.6891**	**0.7359**	**0.8117**	**0.9548**	**1.12181**	**1.3166**	**1.54338**
	Mantari et al.[25]	≠0	0.6014	0.6426	0.6864	0.7329	0.8084	0.951	1.1177	1.3124	1.9394
	Manteri et al.[24]	0	0.6029	0.6443	0.6882	0.635	0.8107	0.9536	1.1204	1.315	1.5415
	TPT [23]	≠0	0.6271	0.6707	0.717	0.7661	0.8452	0.9935	1.1651	1.3637	1.5935
5	**Present**	**0**	**0.5917**	**0.6323**	**0.6755**	**0.7214**	**0.7958**	**0.9360**	**1.0998**	**1.2908**	**1.5131**
	Mantari et al.[25]	≠0	0.5895	0.6299	0.6727	0.7184	0.7923	0.9321	1.0955	1.2865	1.5091
	Manteri et al.[24]	0	0.591	0.6315	0.6746	0.7205	0.7949	0.9347	1.0982	1.289	1.5111
	TPT [23]	≠0	0.6149	0.6577	0.7031	0.7512	0.8287	0.7941	1.1424	1.3372	1.5626
4	**Present**	**0**	**0.5709**	**0.6101**	**0.6518**	**0.6960**	**0.7678**	**0.9031**	**1.0611**	**1.2455**	**1.4600**
	Mantari et al.[25]	≠0	0.5686	0.6075	0.6488	0.6928	0.7641	0.8989	1.0566	1.241	1.456
	Manteri et al.[24]	0	0.57	0.6092	0.6508	0.695	0.7666	0.9016	1.0594	1.2434	1.4576
	TPT [23]	≠0	0.5935	0.6348	0.6785	0.6249	0.7998	0.9401	1.1025	1.2907	1.5084
3	**Present**	**0**	**0.5298**	**0.5662**	**0.6049**	**0.6460**	**0.7126**	**0.8383**	**0.9850**	**1.1562**	**1.3554**

	Mantari et al.[25]	≠0	0.5275	0.5635	0.6018	0.6425	0.7085	0.8335	0.98	1.1514	1.3514
	Manteri et al.[24]	0	0.5288	0.5651	0.6037	0.6447	0.7112	0.08365	0.9828	1.1536	1.3523
	TPT [23]	≠0	0.5514	0.5896	0.6302	0.6733	0.7427	0.873	1.024	1.199	1.4017
2	**Present**	**0**	**0.4363**	**0.4663**	**0.4981**	**0.5320**	**0.5869**	**0.6904**	**0.8113**	**0.9524**	**1.11679**
	Mantari et al.[25]	≠0	0.434	0.4634	0.4947	0.528	0.5822	0.6849	0.8056	0.9473	1.113
	Manteri et al.[24]	0	0.435	0.4649	0.4966	0.5303	0.585	0.6881	0.8085	0.949	1.1125
	TPT [23]	≠0	0.4552	0.4867	0.52	0.5554	0.6126	0.7201	0.8449	0.9898	1.158
1	**Present**	**0**	**0.2075**	**0.2218**	**0.2370**	**0.2532**	**0.2794**	**0.3288**	**0.3865**	**0.4539**	**0.5324**
	Mantari et al.[25]	≠0	0.2063	0.2199	0.2344	0.2499	0.2753	0.324	0.3819	0.4506	0.5317
	Manteri et al.[24]	0	0.2062	0.2204	0.2355	0.2515	0.2774	0.3264	0.3835	0.4502	0.5278
	TPT [23]	≠0	0.2196	0.2345	0.2503	0.2671	0.2944	0.346	0.4065	0.4775	0.5603

Table 8. Comparison of $\overline{\sigma}_{xz}$ for EGPs, a/h=10.

b/a	Theory	ε_{zz}	n=0.1	n=0.3	n=0.5	n=0.7	n=1.0	n=1.5	n=2.0	n=2.5	n=3.0
6	**Present**	**0**	**0.4676**	**0.4667**	**0.4650**	**0.4625**	**0.4571**	**0.4442**	**0.4267**	**0.4048**	**0.37953**
	Mantari et al.[25]	≠0	0.4634	0.4626	0.461	0.4586	0.4536	0.4416	0.4253	0.4065	0.3845
	Manteri et al.[24]	0	0.4633	0.4625	0.4069	0.4585	0.4536	0.4415	0.4252	0.4064	0.3842
	TPT [23]	≠0	0.4776	0.4769	0.4753	0.473	0.4681	0.4564	0.4405	0.4209	0.3981
5	**Present**	**0**	**0.4621**	**0.4613**	**0.4596**	**0.4571**	**0.4518**	**0.4390**	**0.4217**	**0.4001**	**0.37519**
	Mantari et al.[25]	≠0	0.4579	0.4571	0.4556	0.4532	0.4483	0.4364	0.4203	0.4017	0.38
	Manteri et al.[24]	0	0.4579	0.4571	0.4555	0.4531	0.4482	0.4363	0.4202	0.4016	0.3797
	TPT [23]	≠0	0.472	0.4713	0.4697	0.4674	0.4626	0.451	0.4353	0.4159	0.3935
4	**Present**	**0**	**0.4524**	**0.4516**	**0.4500**	**0.4475**	**0.4423**	**0.4298**	**0.4128**	**0.3918**	**0.36734**
	Mantari et al.[25]	≠0	0.4482	0.4475	0.4459	0.4436	0.4388	0.4271	0.4114	0.3933	0.372
	Manteri et al.[24]	0	0.4482	0.4474	0.4458	0.4435	0.4387	0.4271	0.4113	0.3931	0.3717
	TPT [23]	≠0	0.462	0.4613	0.4598	0.4575	0.4528	0.4415	0.4261	0.4071	0.3851
3	**Present**	**0**	**0.4328**	**0.4320**	**0.4304**	**0.4281**	**0.4231**	**0.4112**	**0.3949**	**0.3748**	**0.35145**
	Mantari et al.[25]	≠0	0.4286	0.4279	0.4264	0.4242	0.4196	0.4084	0.3934	0.3761	0.3558
	Manteri et al.[24]	0	0.4285	0.4278	0.4263	0.4241	0.4195	0.4084	0.3933	0.376	0.3555
	TPT [23]	≠0	0.4418	0.4411	0.4396	0.4375	0.433	0.4221	0.4074	0.3893	0.3686
2	**Present**	**0**	**0.3850**	**0.3843**	**0.3829**	**0.3808**	**0.3764**	**0.3658**	**0.3514**	**0.3335**	**0.3128**
	Mantari et al.[25]	≠0	0.381	0.3803	0.379	0.377	0.373	0.363	0.3497	0.3344	0.3165
	Manteri et al.[24]	0	0.3809	0.3803	0.3789	0.377	0.3729	0.363	0.3496	0.3343	0.3162
	TPT [23]	≠0	0.3927	0.3921	0.3908	0.3889	0.3849	0.3752	0.3621	0.346	0.3273
1	**Present**	**0**	**0.2411**	**0.2407**	**0.239**	**0.2385**	**0.2358**	**0.2292**	**0.2202**	**0.2091**	**0.19611**
	Mantari et al.[25]	≠0	0.238	0.2376	0.2368	0.2356	0.233	0.2268	0.2185	0.2094	0.1985
	Manteri et al.[24]	0	0.238	0.2376	0.2368	0.2356	0.233	0.2268	0.2184	0.2093	0.1983
	TPT [23]	≠0	0.2454	0.245	0.2442	0.243	0.2405	0.2344	0.2263	0.2162	0.2045

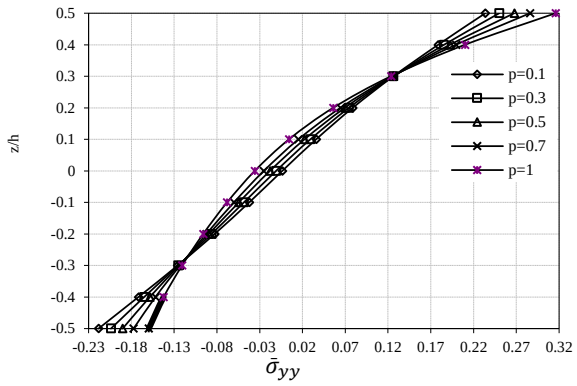

Fig. 5(a). Distribution of $\bar{\sigma}_{yy}$ through the thickness of thick (a/h=4) rectangular (b/a=2) plate.

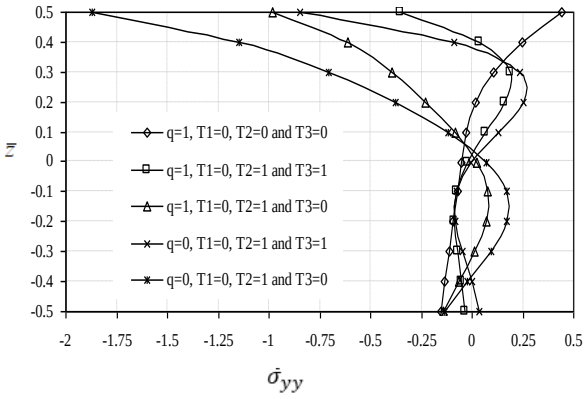

Fig. 5(b). Influence of thermo mechanical loads on $\bar{\sigma}_{yy}$ **,** along the thickness of rectangular (b/a=2) EGP (p=1.5, a/h=2).

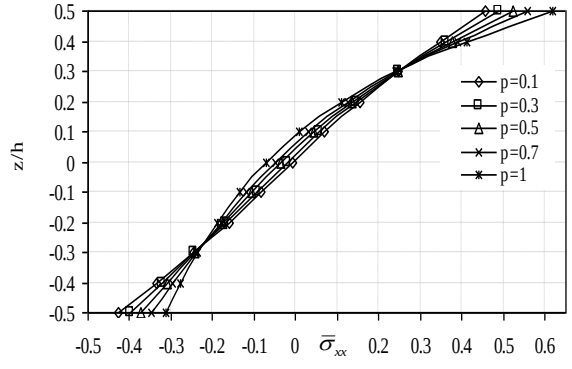

Fig. 6(a). Influence of $\bar{\sigma}_{xx}$ along the thickness of thick (a/h=4) rectangular (b/a=2) plate.

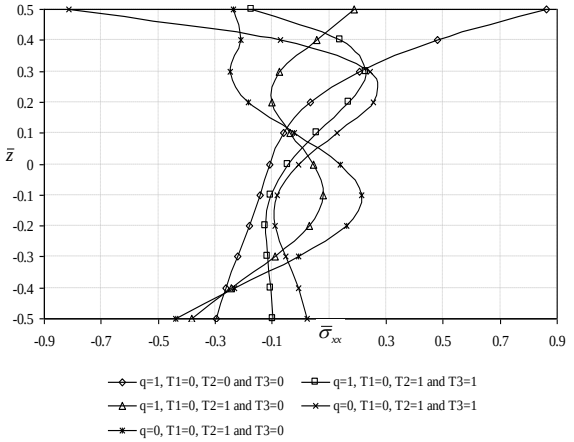

Fig. 6(b). Influence of thermo mechanical loads on $\bar{\sigma}_{xx}$, along the thickness of rectangular (b/a=2) EGP (p=1.5, a/h=2) .

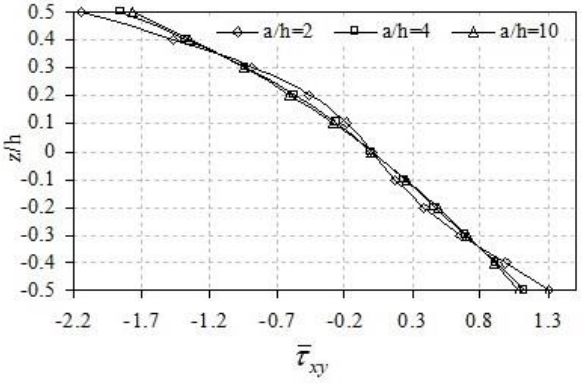

Fig. 7(a). Distribution of $\bar{\tau}_{xy}$ along the thickness of rectangular (b/a=2) EGP (p=0.5).

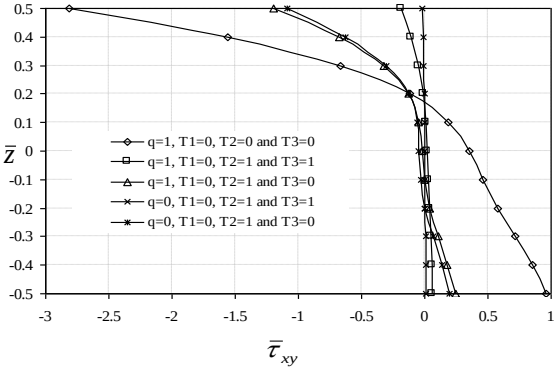

Fig. 7(b). Influence of thermo mechanical loads on $\bar{\tau}_{xy}$ along the thickness of thick (a/h=2) rectangular (b/a=2) EGM plate (p=0.5).

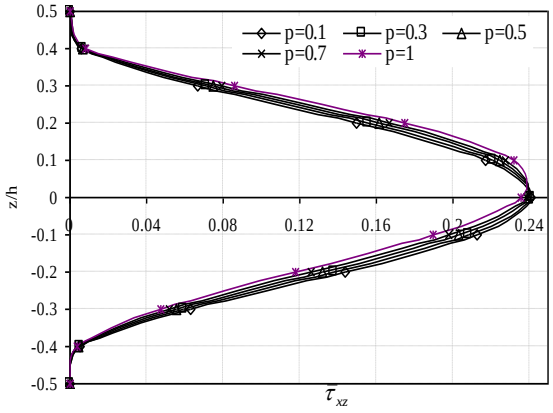

Fig. 8(a). Influence of $\bar{\tau}_{xz}$ along the thickness of square EGP (p=0.5) a/h=10.

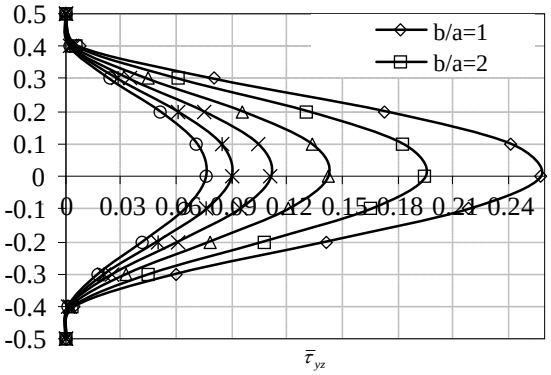

Fig. 8(b). Variaton of $\bar{\tau}_{yz}$ along the thickness of (a/h=2) EGP (p=0.5).

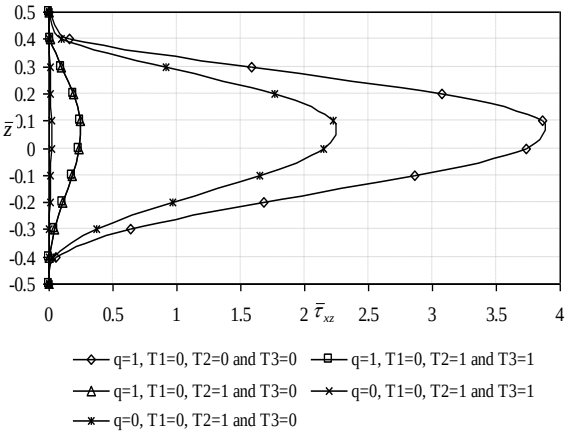

Fig. 8(c). Influence of mechanical & thermal loads on $\bar{\tau}_{xz}$ along the thickness of (a/h=2) rectangular (b/a=2) EGP(p=1.5)

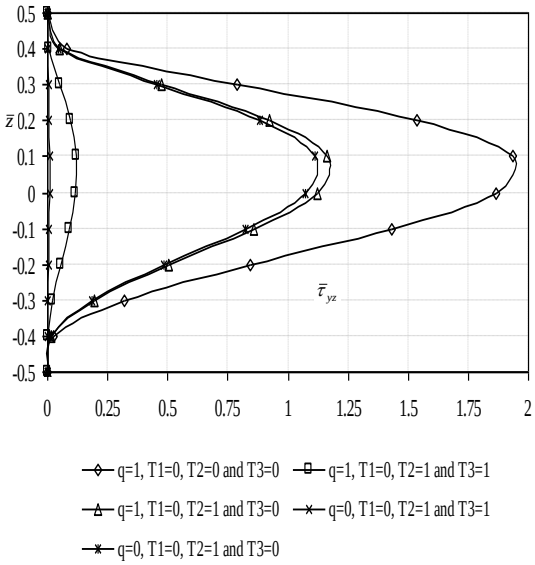

Fig.8(d). Influence of thermo mechanical loads on $\bar{\tau}_{yz}$ along the thickness of thick (a/h=2) rectangular (b/a=2) EGP (p=1.5).

5. Conclusions

The thermomechanical behavior of EGPs is presented based on the new HSDT. The elastic and thermal modulus of the EGPs are changed exponentially along the thickness of the plate. Hamilton's principle is used to get the equations of motion. Closed-form results are obtained for the EGPs under bi-sinusoidal thermomechanical loads with all sides are simple support using the inverse method. From the numerical results, it can be inferred that the present novel theory without including the stretching effect estimates the displacements and stresses of the EGPs accurately with the well-known HPT [23], TPT [23], and Mantari et al. [24]. The gradients or inhomogeneities in materials play a vital role in estimating the bending behavior of the EGPs. The change of elastic modulus and thermal modulus in the thickness of the plate exponentially can avoid interface problems, and hence the stress variation is smooth. The analytical formulations and solutions presented in this paper should help in extending investigations and should provide the engineers with the potential for the design and development of exponentially graded plates for advanced engineering applications.

Appendix

$$S_{11} = A_{11}\alpha^2 + A_{33}\beta^2$$
$$S_{12} = (A_{12} + A_{33})\alpha\beta;$$
$$S_{13} = -B_{11}\alpha^3 - (B_{12} + 2B_{33})\alpha\beta^2;$$
$$S_{14} = (f^* B_{11} + E_{11})\alpha^2 + (f^* B_{33} + E_{33})\beta^2;$$
$$S_{15} = (f^* B_{12} + E_{12} + f^* B_{33} + E_{33})\alpha\beta;$$
$$S_{21} = (A_{21} + A_{33})\alpha\beta;$$
$$S_{22} = A_{22}\beta^2 + A_{33}\alpha^2;$$
$$S_{23} = -(B_{21} + 2B_{33})\alpha^2\beta - B_{22}\beta^3;$$
$$S_{24} = (f^* B_{21} + E_{21} + f^* B_{33} + E_{33})\alpha\beta;$$
$$S_{25} = (f^* B_{33} + E_{33})\alpha^2 + (f^* B_{22} + E_{22})\beta^2;$$
$$S_{31} = B_{11}\alpha^3 + (B_{21} + 2B_{33})\alpha\beta^2;$$
$$S_{32} = B_{22}\beta^3 + (B_{12} + 2B_{33})\alpha^2\beta;$$
$$S_{33} = -D_{11}(\alpha^4 + \beta^4) - (2D_{12} + 4D_{33})\alpha^2\beta^2;$$
$$S_{34} = (D_{11} f^* + F_{11})\alpha^3$$
$$+ (D_{21} f^* + F_{21} + 2 f^* D_{33} + F_{33})\alpha\beta^2;$$
$$S_{35} = (D_{22} f^* + F_{22})\beta^3$$
$$+ (D_{12} f^* + F_{12} + 2 f^* D_{332} + F_{33})\alpha^2\beta;$$
$$S_{41} = (B_{11} f^* + E_{11})\alpha^2 + (B_{33} f^* + E_{33})\beta^2;$$
$$S_{42} = (B_{12} f^* + f^* B_{33} + E_{12} + E_{33})\alpha\beta;$$
$$S_{43} = -(f^* D_{11} + F_{11})\alpha^3$$
$$-(f^* D_{12} + 2 f^* D_{33} + F_{12} + 2F_{33})\alpha\beta^2;$$
$$S_{44} = (f^{*2} D_{11} + 2 f^* F_{11} + H_{11})\alpha^2$$
$$+ (f^{*2} D_{33} + 2 f^* F_{33} + H_{33})\beta^2$$
$$+ J_{11} f^{*2} + K_{11} f^* + L_{11} f^* + M_{11}$$
$$S_{45} = (f^{*2} D_{12} + 2 f^* F_{12} + H_{12} + H_{33}$$
$$+ f^{*2} D_{33} + 2 f^* F_{33})\alpha\beta \quad ;$$
$$S_{51} = (B_{12} f^* + f^* B_{33} + E_{12} + E_{33})\alpha\beta;$$
$$S_{52} = (B_{33} f^* + E_{33})\alpha^2 + (B_{11} f^* + E_{11})\beta^2;$$
$$S_{53} = -(f^* D_{11} + F_{11})\beta^3$$
$$-(f^* D_{12} + 2 f^* D_{33} + F_{12} + 2F_{33})\alpha^2\beta;$$
$$S_{54} = (f^{*2} D_{12} + 2 f^* F_{12} + H_{12} +$$
$$H_{33} + f^{*2} D_{33} + 2 f^* F_{33})\alpha\beta$$
$$S_{55} = (f^{*2} D_{11} + 2 f^* F_{11} + H_{11})\beta^2$$
$$+ (f^{*2} D_{33} + 2 f^* F_{33} + H_{33})\alpha^2 + J_{11} f^{*2}$$
$$+ K_{11} f^* + L_{11} f^* + M_{11}$$

$$[F] = \begin{bmatrix} -\alpha N^T_{xx}, -\beta N^T_{yy}, -q - \alpha^2 M^T_{xx} \\ -\beta^2 M^T_{yy}, \alpha(f^* M^T_{xx} + P^T_{xx}), \\ \beta(f^* M^T_{yy} + P^T_{yy}) \end{bmatrix}$$

References

[1] J. N. Reddy and C. D. Chin, "Thermomechanical analysis of functionally graded cylinders and plates". *J. Therm. Stresses.*, Vol. 21, No. 6, pp. 593-626, (1998).

[2] A. M. Zenkour, "A comprehensive analysis of functionally graded sandwich plates: Part-1-Deflection and stresses". *Int. J. Solids Struct.*, Vol. 42, No. 18-19, pp. 5224-5242, (2005).

[3] A. M. Zenkour, "A comprehensive analysis of functionally graded sandwich plates: Part-2-Buckling and free vibration". *Int. J. Solids Struct.*, Vol. 42, No. 18-19, pp. 5243-5258, (2005).

[4] A. M. Zenkour, "Generalized shear deformation theory for bending analysis of functionally graded plates". *Appl. Math. Model.*, Vol. 30, No. 1, pp. 67-84, (2006).

[5] B. N. Pandya and T. Kant, "Higher-order shear deformable theories for flexure of sandwich plates-finite element evaluations". *Int. J. Solids Struct.*, Vol. 24, No. 12, pp. 1267-1286, (1988).

[6] B. N. Pandya and T. Kant, "Finite element analysis of laminated composite plates using a higher order displacement model". *Compos. Sci. Technol.*, Vol. 32, No. 2, pp.137-155, (1988).

[7] T. Kant and K. Swaminathan, "Analytical solutions for the static analysis of laminated composite and sandwich plates

based on higher order refined theory". *Compos. Struct.*, Vol. 56, No. 4, pp. 329-344, (2002).

[8] T. Kant and K. Swaminathan, "Analytical solutions for free vibration analysis of laminated composite and sandwich plates based on higher order refined theory". *Compos. Struct.*, Vol. 53, No. 1, pp. 73-85, (2001).

[9] A. K. Garg, R. K. Khare and T. Kant, "Higher order closed form solutions for free vibration of laminated composite and sandwich shells". *J. Sandw. Struct. Mater.*, Vol. 8, No. 3, pp. 205-235, (2006).

[10] M. E Golmakani and M. Kadkhodayan, "Nonlinear bending analysis of annular FGM plates using higher order shear deformation plate theories". *Compos. Struct.*, Vol. 93. No. 2, pp. 973-982, (2011).

[11] H. Matsunaga, "Free vibration and stability of functionally graded plates according to a 2-D higher-order deformation theory". *Compos. Struct.*, Vol. 82, No. 2, pp. 499-512, (2008).

[12] H. Matsunaga, "Stress analysis of functionally graded plates subjected to thermal and mechanical loadings". *Compos. Struct.*, Vol. 87, No. 4, pp. 344-357, (2009).

[13] S. Xiang and G. Kang, "A nth-order shear deformation theory for the bending analysis on the functionally graded plates". *Eur. J. Mech. A-Solid*, Vol. 37, pp.336-343, (2013).

[14] J. Suresh Kumar, B. Sidda Reddy, C. Eswara Reddy and K. Vijaya Kumar Reddy, "Nonlinear Thermal Analysis of Functionally Graded Plates Using Higher Order Theory", *Innovat Syst. Des. Eng.*, Vol. 2, No. 5, pp. 1-13, (2011).

[15] B. Sidda Reddy, J. Suresh Kumar, C. Eswara Reddy and K. Vijaya Kumar Reddy, "Buckling Analysis of Functionally Graded Material Plates Using Higher Order Shear Deformation Theory", *J. Compos.*, Vol. 2013, Article ID 808764, 12 pages, (2013).

[16] J. Suresh Kumar, B. Sidda Reddy and C. Eswara Reddy, "Nonlinear bending analysis of functionally graded plates using higher order theory". *Int. J. Eng. Sci. Technol.*, Vol. 3, No. 4, pp. 3010-3022, (2011).

[17] T. Mohammad and B. N. Singh, "Thermo-mechanical deformation behavior of functionally graded rectangular plates subjected to various boundary conditions and loadings" *Int. J. Aerosp. Mech. Eng.*, Vol. 6, No. 1, pp. 14-25, (2012).

[18] A. M. Zenkour and N. A. Alghamdi, "Bending analysis of functionally graded sandwich plates under the effect of mechanical and thermal loads". *Mech. Adv. Mate. Struc.*, Vol. 17, No. 6, pp. 419-432, (2010).

[19] H. A. Mechab, A. Ismail, H. A. Belhadej and A. E. A. Bedia, "A two variable refined plate theory for the bending analysis of functionally graded plates". *Act. Mech. Sin.*, Vol. 26, No. 6, pp. 941-949, (2010).

[20] E. Carrera, S. Brischetto, M. Cinefra and M. Soave, "Effects of thickness stretching in functionally graded plates and shells". *Compos. B. Eng.*, Vol. 42, No. 2, pp. 123-133, (2011).

[21] T. H. D. A. Henni, A. Tounsi and A. B. E. Abbes, "A New Hyperbolic Shear Deformation Theory for Bending Analysis of Functionally Graded Plates". *Model. Simu. Eng.*, Vol. 2012, pp. 1-10, (2012).

[22] A. M. A. Neves, A. J. M. Ferreira, E. Carrera, M. Cinefra, C. M. C. Roque and R. M. N. Jorge, "A quasi-3d sinusoidal shear deformation theory for the static and free vibration analysis of functionally graded plates". *Compos. B. Eng.*, Vol. 43, No. 2, pp. 711-725, (2012).

[23] A. M. Zenkour, "Benchmark trigonometric and 3-D elasticity solutions for an exponentially graded thick rectangular plate". *Appl. Math. Model.*, Vol. 77, No. 4, pp. 197-214, (2007).

[24] J. L. Mantari and C. Guedes Soares, "Bending analysis of thick exponentially graded plates using a new trigonometric higher order shear deformation theory". *Compos. Struct.*, Vol. 94, No. 6, pp. 1991-2000, (2012).

[25] J. L. Mantari and C. Guedes Soares, "A novel higher-order shear deformation theory with stretching effect for functionally graded plates". *Compos. B. Eng*., Vol. 45, No. 1, pp. 268–281, (2013).

[26] A. M. A. Neves, A. J. M. Ferreira, E. Carrera, M. Cinefra, C. M. C. Roque, R. M. N. Jorge and C. M. M. Soares, "Static, free vibration and buckling analysis of isotropic and sandwich functionally graded plates using a quasi-3D higher-order shear deformation theory and a meshless technique". *Compos. B. Eng*., Vol. 44, No. 1, pp. 657–674, (2013).

[27] G. N. Praveen and J. N. Reddy, "Nonlinear transient thermo elastic analysis of functionally graded ceramic-metal plates". *Int. J. Solids Struct.*, Vol. 35, No. 33, pp. 4457-4476, (1998).

[28] A. Attia, A. A. Bousahla, A. Tounsi, S. R. Mahmoud and A. S. Alwabl, "A refined four variable plate theory for thermoelastic analysis of FGM plates resting on variable elastic foundations", *Struct. Eng. Mech.*, Vol. 65, No. 4, pp. 453-464, (2018).

[29] A. Fahsi, A. Tounsi, H. Hebali, A. Chikh, E. A. A. Bedia and S. R. Mahmoud, "A four variable refined nth-order shear deformation theory for mechanical and thermal buckling analysis of functionally graded plates", *Geomech. Eng.*, Vol. 13, No. 3, pp. 385-410, (2017).

[30] A. Chikh, A. Tounsi, H. Hebali and S. R. Mahmoud, "Thermal buckling analysis of cross-ply laminated plates using a simplified HSDT", *Smart Struct. Systems*., Vol. 19, No. 3, pp. 289-297, (2017).

[31] F. El-Haina, A. Bakora, A. A. Bousahla, A. Tounsi and S. R. Mahmoud, "A simple analytical approach for thermal buckling of thick functionally graded sandwich plates", *Struct. Eng. Mch.*, Vol. 63, No. 5, pp. 585-595, (2017).

[32] A. Menasria, A. Bouhadra, A. Tounsi, A. A. Bousahla and S. R. Mahmoud, , "A new and simple HSDT for thermal stability analysis of FG sandwich plates", *Steel Compos Struct*, Vo. 25, No. 2, pp. 157-175, (2017).

[33] Y. Beldjelili, A. Tounsi and S. R. Mahmoud, "Hygro-thermo-mechanical bending of S-FGM plates resting on variable elastic foundations using a four-variable trigonometric plate theory", *Smart Struct. Syst.*, Vol. 18, No. 4, pp. 755-786, (2016).

[34] S. Boutaleb, K. H. Benrahou, A. Bakora, A. Algarni, A. A. Bousahla, A. Tounsi, and S. R. Mahmoud, "Dynamic analysis of nanosize FG rectangular plates based on simple nonlocal quasi 3D HSDT", *Adv. Nano Res.*, Vol. 7, No. 3, pp.189-206, (2019).

[35] Z. Boukhlif, M. Bouremana, F. Bourada, A. A. Bousahla, M. Bourada, A. Tounsi and M. A. Al-Osta, "A simple quasi-3D HSDT for the dynamics analysis of FG thick plate on elastic foundation", *Steel. Compos. Struct.*, Vol. 31, No. 5, pp. 503-516, (2019).

[36] S. Bouanati, K. H. Benrahou, A. A. Hassen, A. Y. Sihame, F. Bernard, A. Tounsi and E. A. A. Bedia, "Investigation of wave propagation in anisotropic plates via quasi 3D HSDT", *Geomech. Eng.*, Vol. 18, No. 1, pp. 85-96 (2019).

[37] A. A. Hassen, A. Tounsi and F. Bernard, "Effect of thickness stretching and porosity on mechanical response of a functionally graded beams resting on elastic foundations". *Int. J. of Mech Mater Des*., Vol. 13, No. 1, pp. 71-84, (2017).

[38] A. Benahmed, M. S. A. Houari, S. Benyoucef, K. Belakhdar and A. Tounsi, "A novel quasi-3D hyperbolic shear deformation theory for functionally graded thick rectangular plates on elastic foundation", *Geomech. Eng.*, Vol. 12, No. 1, pp. 9-34, (2017).

[39] B. Karami, M. Janghorban, D. Shahsavari and A. Tounsi, "A size-dependent quasi-3D model for wave dispersion analysis of FG nanoplates", *Steel Compos. Struc.*, Vol. 28, No. 1, pp. 99-110, (2018).

[40] F. Z. Zaoui, O. Djamel and A. Tounsi, "New 2D and quasi-3D shear deformation theories for free vibration of functionally graded plates on elastic foundations",

Compos. B. Eng., Vol. 159, pp. 231-247, (2019).

[41] A. Bouhadra, A. Tounsi, A. A. Bousahla, S. Benyoucef and S. R. Mahmoud, "Improved HSDT accounting for effect of thickness stretching in advanced composite plates", *Struct. Eng. Mech.* Vol. 6, No. 1, pp. 61-73, (2018).

[42] A. Younsi, A. Tounsi, F. Z. Zaoui, A. A. Bousahla and S. R. Mahmoud, "Novel quasi-3D and 2D shear deformation theories for bending and free vibration analysis of FGM plates", *Geomech. Eng.*, Vol. 14, No. 6, pp. 519-532, (2018).

[43] M. Abualnour, M.S.A. Houari, A. Tounsi, E. A. A. Bedia and S. R. Mahmoud, "A novel quasi-3D trigonometric plate theory for free vibration analysis of advanced composite plates", *Compos. Struct.*, Vol. 184, pp. 688-697, (2017).

How to cite this paper:

Bathini Sidda Reddy, Ch. Ravikiran and K. Vijaya Kumar Reddy, "Bending of exponentially graded plates using new HSDT," *J. Comput. Appl. Res. Mech. Eng.*, Vol. 11, No. 1, pp. 257-277, (2021).

DOI: 10.22061/JCARME.2020.6370.1809

URL: https://jcarme.sru.ac.ir/?_action=showPDF&article=1474